A Novel Fluidic Control System for Stacked Rapid Sand Filters

Michael J. Adelman[1]; Monroe L. Weber-Shirk, Ph.D., M.ASCE[2]; Jeffrey C. Will[3]; Anderson N. Cordero[4]; William J. Maher[5]; and Leonard W. Lion, Ph.D.[6]

Abstract

Infrastructure for water treatment faces numerous challenges around the world, including the high failure rate of digital, electronic, pneumatic, and mechanical control systems due to their large number of components and their dependency on proprietary parts for repair. The development of more efficient, reliable, easily-repaired water treatment controls that rely on simple fluidics rather than on sophisticated systems has the potential to significantly improve the reliability of drinking water treatment plants, particularly for cities and towns in developing countries. The AguaClara stacked rapid sand filter (SRSF) has been proposed as a more robust and sustainable alternative to conventional rapid sand filters because each filter can backwash at the same flow rate used for filtration without requiring pumps or storage tanks. The viability of stacked rapid sand filtration has been demonstrated through previous laboratory studies and at a municipal water treatment plant. This paper presents a novel control system for the SRSF based on fluidics. The fluidic control system, which permits changing between the filtration and backwash modes of operation with a single valve, was developed in the laboratory and applied in the first full-scale SRSF. The water level in the filter is regulated by a siphon pipe, which conveys flow during backwash and

[1]Graduate student, School of Civil and Environmental Engineering, Hollister Hall, Cornell University, Ithaca, NY, 14853. Email: mja233@cornell.edu

[2]Senior lecturer, School of Civil and Environmental Engineering, Hollister Hall, Cornell University, Ithaca, NY, 14853 (corresponding author). Email: mw24@cornell.edu

[3]Fulbright fellow, Agua Para el Pueblo, Tegucigalpa, M.D.C., F.M., Honduras. Email: jeffrey-will122@gmail.com

[4]Systems consultant, Accenture, 1345 Ave of the Americas, New York, NY, 10105. Email: anc26@cornell.edu

[5]Undergraduate student, School of Civil and Environmental Engineering, Hollister Hall, Cornell University, Ithaca, NY, 14853. Email: wjm96@cornell.edu

[6]Professor, School of Civil and Environmental Engineering, Hollister Hall, Cornell University, Ithaca, NY, 14853. Email: LWL3@cornell.edu

which contains an air trap to block flow during filtration. The state of the siphon pipe and the ensuing state of the filter is controlled by one small-diameter air valve.

CE Database Subject Headings: Sand, Filter; Water treatment; Drinking water; Municipal water; Backwashing; Sustainable development; Control systems; Flow control

INTRODUCTION

In many cities and towns, drinking water infrastructure is inadequate, under-performing, or technically deficient (Lee and Schwab, 2005). Failure of water treatment systems is part of the reason why an estimated 1.8 billion people lack access to safe drinking water (Onda et al., 2012). Moreover, the high capital and operating costs of water treatment systems have been identified as major barriers to their more widespread implementation in developing countries (Hokanson et al., 2007). In industrialized countries, water treatment systems are more widely available, but there is nevertheless a significant need of capital for maintenance and for new water infrastructure in the coming decades (ASCE, 2009).

Water treatment plants that rely on digital, electronic, pneumatic, and mechanized control systems have multiple failure modes that result in a short mean time between repair events. The failures of mechanized plants are due to component failures, reliance on proprietary parts that are unavailable in the local supply chains, high energy costs, and designs that fail to provide adequate feedback to the operator for successful water treatment. For example, 20 modular mechanized water treatment plants were installed in Honduran cities in a program that ended in 2008. By the beginning of 2012, 50% of the plants had been abandoned due to control system failures and significant energy costs [Smith, D.W., 2012, Agua Para el Pueblo-Honduras, personal communication].

The choice of technology is a crucial factor to achieve sustainability for water projects (Breslin, 2003), and the use of technology that is inappropriate for its context has been implicated as the reason for many failures of infrastructure systems (Moe and Rheingans, 2006). Water treatment plants can be designed for sustainable operation and a long useful life by simplifying the control system, eliminating dependence on electricity, minimizing the number of moving parts, designing the unit processes to provide operator feedback, using locally available materials, and simplifying operation and maintenance procedures. Although water treatment plant mechanization and automation might normally be expected to reduce labor requirements and thus operating costs, the need for highly skilled professionals with different expertise to maintain the control systems of automated plants may actually increase labor costs. In addition, the parts required for automated systems are not readily available in many areas of the world.

The need for resilient water treatment plant designs that are high-performing with low capital and operating costs led to the search for an improved filtration design by the AguaClara program at Cornell University in 2010. Initial evaluation of existing technologies revealed none meeting these requirements. Slow sand filters require too much level land (a scarce resource in mountainous terrain) to treat large flow rates, and rapid sand filters require either enclosed filter vessels, pumps, large storage tanks, or sets of six filters working together to achieve the high velocities required for backwash. The capital costs of the rapid sand filter options are high, often out of reach for small to mid-size communities, and the closed-vessel pressure filter option does not give plant operators visual feedback on the condition of the filtration system. For this reason, pressure filters are not considered appropriate for normal surface water treatment, and design guidelines limit their use to iron and manganese removal (WSCGL, 2007).

The AguaClara stacked rapid sand filter (SRSF) was invented to address the need for a robust, lower cost, high-performing, and sustainable alternative to conventional rapid sand filters (Adelman et al., 2012). The SRSF uses the same flow rate for the filtration and backwash cycles, and it therefore does not require the pumps or elevated storage tanks needed to backwash conventional filters. The SRSF works by placing inlets and outlets made of well-screen pipe within the filter sand bed, creating multiple layers that filter in parallel but that are backwashed in series. This allows the SRSF to achieve a backwash velocity equal to the number of layers times the filtration velocity with the same flow entering the filter. The typical design ranges of filtration and backwash velocities for rapid sand filtration differ by approximately a factor of six, making six filter layers a reasonable choice for design. Flow through the bed of a six-layer SRSF during the filtration and backwash cycles is shown in Figure 1.

The viability of the SRSF was first demonstrated through laboratory studies and a small-scale field demonstration by Adelman et al. (2012), and the first generation full-scale 12 L/s SRSF was built in 2011 at the municipal water plant serving the town of Támara, Francisco Morazán, Honduras (Will et al., 2012). The initial report of the SRSF by Adelman et al. (2012) discussed the requirement for flow to be provided to the layers of the sand bed as shown in Figure 1, but no control system was proposed to achieve this. This paper presents a novel system of fluidics to control the SRSF, supported by theoretical analysis, experimental demonstrations, and full-scale implementation. This system consists of inlet and outlet boxes with riser pipes and a siphon with an air valve to control the mode of operation. The fluidic control system eliminates the need for digital, electronic, pneumatic, or other mechanized controls and allows the operator to select the cycle of operation of the filter with a single small-diameter air valve.

MATERIALS AND METHODS

Pilot-scale apparatus

A pilot-scale apparatus (Figure 2) was developed for laboratory studies of the proposed fluidic control system, starting from the apparatus used by Adelman et al. (2012) for the original proof-of-concept studies. The SRSF in this system was built in a 4" (10.16 cm) diameter clear PVC column with six 20 cm layers. The inlet and outlet pipes were 1/2" (1.27 cm) PVC with 0.2 mm well-screen slots spaced at 1/8" (0.318 cm) provided by Big Foot Mfg. in Cadillac, MI. The sand bed consisted of typical rapid sand filter sand, with an effective size of 0.45 mm and a uniformity coefficient of 1.4 (Ricci Bros. Sand Co., Port Norris, NJ). Water was applied to this filter at a total flow rate of 5.3 L/min, giving a backwash velocity of 11 mm/s when the flow passed through all layers in series and a filtration velocity of 1.83 mm/s when the flow was divided among the six layers. These values are consistent with typical design values for filtration and backwash velocities in single-media rapid sand filters (Reynolds and Richards, 1996).

The experimental apparatus also included fluidic controls to set the mode of operation of the SRSF by controlling air entry to and exit from a siphon system. Important components of this fluidic control system are shown in Figure 2, including an inlet box where water enters the SRSF from upstream processes, an outlet box for filtered water, a backwash siphon, and an air valve. These components regulate the water levels and flow paths during each cycle of operation.

Control of parameters and data acquisition

Raw water for the laboratory apparatus came from a temperature-controlled reservoir which blended hot and cold tap water to achieve a room-temperature mix. This prevented excess dissolved gases in the cold tap water from influencing the hydraulics of the system. The tap water came from the Cornell University water system, and had an average pH of 7.7 with roughly 150 mg/L as $CaCO_3$ of hardness and 120 mg/L as $CaCO_3$ of alkalinity (Foote et al., 2012). The pump shown in Figure 2 was used along with a flow control valve to supply water to the inlet box at a constant rate of 5.3 L/min. In the municipal-scale filter discussed below, the inlet box is gravity-fed by placement just below the sedimentation tank outlet, and no pumping of water is required.

Important water levels in the system were tracked using differential pressure sensors (PX26 series, Omega Engineering Inc., Bridgeport, NJ). These sensors were installed at the locations indicated in Figure 2, with their positive side connected via fittings to the inlet box or filter column and their negative side exposed to the atmosphere to correct for variations in atmospheric pressure. The sensors were calibrated to measure pressure in units of centimeters of water, so that the water level could be tracked in the inlet box and the filter column during experiments. Data from these pressure sensors was logged to a computer via the laboratory process control and data acquisition system described by Weber-Shirk (2009).

RESULTS AND DISCUSSION

Overall control system

The SRSF fluidic control system uses the backwash siphon to set the water level in the filter and thereby control the mode of operation (Figure 3). Only one valve is required to operate this filter - the air valve used to fill or empty the siphon pipe by establishing or releasing an air trap.

When the siphon pipe is blocked by air, the SRSF is in filtration mode. Water is forced to exit over the weir in the outlet box, and the water level in the inlet box and in the filter are high enough to overcome the filtration head loss HL_{Filter}. This head loss is attributable to flow through the inlet and outlet plumbing, slotted pipes, and sand bed along any one of the six parallel paths through the filter. The clean bed head loss during the filtration cycle can be estimated with familiar models such as the Carmen-Kozeny equation or the Rose equation (see, for example, Reynolds and Richards, 1996).

When there is water flow in the siphon, the SRSF is in backwash mode. The water level in the filter is just high enough for flow to pass through the siphon and exit the system over the backwash weir. The water level in the inlet box drops until it provides the total required backwash head loss HL_{BW}. The head h_L required to fluidize a sand bed of depth H_{Sand} is given by Equation (1):

$$h_L = H_{Sand}\left(1-\varepsilon\right)\left(\frac{\rho_{Sand}}{\rho_{Water}}-1\right) \tag{1}$$

where ε is the porosity of the sand, ρ_{Sand} is the sand density, ρ_{Water} and is the density of water. Based on both typical properties of filtration sand and on experimental observation, h_L is approximately equal to the depth of the sand bed in both conventional and stacked rapid sand filters (Adelman et al., 2012). Note that the total backwash head loss also includes losses in the inlet plumbing or siphon pipe. The riser pipes on the entrance to the top three inlets prevent these inlets from receiving flow during backwash, causing all flow to be directed to the bottom inlet in order to fluidize the sand media and backwash the filter.

Experimental evidence of mode transitions

The effectiveness of the fluidic control system to set the mode of operation of the filter was confirmed using the laboratory apparatus. Figure 4 shows the temporal variation of the water level in the inlet box and the filter column as the control system was used to set both cycles. In the experiment shown, the SRSF started in filtration mode, was changed to backwash, and then was returned to filtration. Water levels in the figure are measured relative to the top of the settled sand bed.

The data presented in Figure 4 is divided into five "zones" illustrating the important steps in the transition between filtration and backwash cycles using the fluidic control system:

- *Zone A.* The system is in filtration mode, with the water level high enough in both the inlet box and the filter column for flow to exit over the outlet weir. The inlet box level is a few centimeters above the water level in the filter column, which represents the head loss in the inlet plumbing. The top of the siphon pipe is completely submerged by the water in the filter column, but is maintaining an air trap to prevent water from escaping to the backwash weir.
- *Zone B.* The air valve is opened and then closed over an interval of approximately 5 s. This time interval is also used in the full-scale SRSF. Opening the air valve allows the trapped air to escape, so that the siphon can fill and water can begin flowing out over the backwash weir. Once there is flow in the siphon, the water level quickly drops from its former level above the siphon pipe in both the filter and the inlet box. This transition takes about 1 minute in the laboratory filter and about 3 minutes in the field.
- *Zone C.* The system is in backwash mode. The water level in the filter column is a few centimeters above the elevation of the backwash weir, representing the head loss in the siphon pipe. The water level in the inlet box is high enough to provide the 1.2 m backwash head loss (equal to the depth of the sand bed), but below the top of the

highest three riser pipes. This directs all flow from the inlet box to the bottom inlet of the filter.

- *Zone D.* The air valve is opened and then closed, again for about 5 s in the lab and the field. This allows air to be pulled into the siphon, cutting off flow in the siphon pipe and re-forming the air trap. Because the water can no longer exit via the backwash siphon, it must rise in both the inlet box and the filter column so it can once again exit over the outlet weir. The elevation of the riser pipes in the inlet box is evidenced by the short horizontal section on the trace of the inlet box water level, between about 12 and 14 minutes of run time.
- *Zone E.* The system has returned to filtration mode. Once again, the height of water in the filter column reflects the elevation of the outlet weir plus the clean-bed filtration cycle head loss.

This data in Figure 4 provide good evidence that the fluidic control system works as proposed. The effectiveness of this control system was also confirmed by the success of the SRSF in the field. The first full-scale SRSF in Támara can successfully transition between filtration and backwash just as was observed in the pilot-scale system (Will et al., 2012).

Fluidic control of the mode of operation

Controls based on fluidics are used to select which inlets and outlets are active during filtration and backwash modes. Flow to the top three inlets must cease during backwash so that all of the water is forced into the bottom of the filter. The top three inlets are turned off by lowering the water in the inlet box to be below the level of the three inlets, as shown in Figure 3(b). It is also important that outlet pipes not be hydraulically connected during backwash, to prevent backwash water from preferentially traveling through the pipes instead of through the fluidized sand bed. The outlet pipes are disconnected from each other by lowering the water level in the outlet box to be below the top of the outlet pipes.

The successful transition in flow was based on an analysis to determine the relevant head losses in the system. The placement of the inlet box and the length of the riser pipes depend on both the filtration and backwash cycle head losses. In addition, the energy losses between the entrance to the bottom inlet manifold and the siphon exit can be used to estimate where the water levels will be in the unused inlet and outlet pipes during backwash. The water levels in these pipes are illustrated in Figure 3(b), and the outlet box must be placed as shown in the figure to prevent short-circuiting during backwash.

Changes in water levels in the transition from filtration to backwash mode are set by the siphon and controlled by the air valve. To initiate backwash, the air valve opens the siphon pipe, closes three inlet pipes, closes three outlet pipes, and increases the flow rate through the bottom filter inlet. To initiate filtration, the air valve closes the siphon pipe, opens three inlet pipes, and opens three outlet pipes. The use of fluidics thus eliminates seven large-diameter valves - one on each inlet pipe and each outlet pipe - that would otherwise be required to control filter operation.

Backwash siphon air trap hydrostatics

The siphon pipe and its air trap are the central elements of the SRSF fluidic system, and the design of this siphon pipe is critical to the operation of the control system. The hydrostatics of the SRSF siphon were characterized in the laboratory apparatus. Figure 5 shows the siphon during backwash mode, the initial air volume that is taken into the pipe just after the air valve is opened to cut off backwash flow, and the hydrostatic equilibrium observed during the filtration cycle.

At the end of the backwash cycle, the siphon is broken by opening the air valve. Because the siphon is under negative gauge pressure when it is conveying backwash water, as in Figure 5(a), air will enter the pipe when the air valve is opened. The initial volume of air that is pulled into the siphon pipe at the end of the backwash cycle occupies the lengths L_1, L_2, and L_3 in the siphon pipe, as shown in Figure 5(b). As the SRSF transitions to filtration mode and the water level rises (Zone D in Figure 4), this air volume is pushed along the siphon into the position shown in Figure 5(c).

The siphon pipe geometry must be designed so that the air trap can be maintained as the water level rises in the filter box. The lower U-shaped portion of the siphon pipe remains filled with water that acts as a "water seal," and the back pressure on this side of the pipe must be sufficient to resist the pressure exerted on the air trap by the water in the filter column. The density of air is sufficiently small compared to the density of water that the pressure can be assumed to be constant in the air trap, so the hydrostatic pressures at points 1 and 2 in Figure 5(c) must balance:

$$P_1 = P_2 = \rho_{Water} g H_1 + P_{Atm} \tag{2}$$

where P_1 and P_2 are the absolute pressures at points 1 and 2, P_{Atm} is atmospheric pressure, ρ_{Water} is the density of water, g is the gravitational acceleration, and H_1 is the length defined in Figure 5(c). Because the pressures balance as shown in Equation (2), the difference in height from the water in the filter column to point 1 and the vertical displacement of the water seal from the backwash weir to point 2 will have an identical value H_1. The increase in hydrostatic pressure will cause the air in the trap to compress slightly from its initial volume:

$$P_{Atm} V_{Initial} = P_1 V_{Compressed} \tag{3}$$

where $V_{Initial}$ is the initial air volume and $V_{Compressed}$ is the volume of the air trap in its compressed state. From the geometry of the system, the initial volume in the air trap is approximately:

$$V_{Initial} = A_{Siphon} \left(L_1 + L_2 + L_3 \right) \tag{4}$$

where A_{Siphon} is the cross-sectional area of the siphon pipe and L_1, L_2, and L_3 are the pipe lengths defined in Figure 5(b). Note that this initial air volume is conservatively taken to exclude the length L_0 that remains submerged as a result of the water level in the column during backwash. Once the water has risen in the filter as in Figure 5(c), the air volume is:

$$V_{Compressed} = A_{Siphon}\left(L_2 + L_3 + H_1 + H_2\right) \tag{5}$$

where H_2 is the distance between the water level in the upstream side of the siphon pipe and the horizontal section of the siphon pipe.

The system of Equations (2) through (5) can be used to analyze the equilibrium condition in the siphon pipe at any point during filtration. Substituting Equations (2), (4), and (5) into Equation (3) and dividing through by A_{Siphon} gives:

$$P_{Atm}\left(L_1 + L_2 + L_3\right) = \left(\rho_{Water} g H_1 + P_{Atm}\right)\left(L_2 + L_3 + H_1 + H_2\right) \tag{6}$$

A useful result of Equation (6) is that it is possible to solve for the position of water levels in the siphon pipe, given the height of water in the filter, H_{Rise}. In order to do this, H_2 is defined geometrically as:

$$H_2 = L_0 + L_1 - \left(H_{Rise} - H_1\right) \tag{7}$$

where H_{Rise} is the height of water in the filter from the inlet of the siphon pipe. If the water in the column has risen by a given amount H_{Rise}, Equation (7) can be substituted into Equation (6) to eliminate all unknowns except for H_1:

$$P_{Atm}\left(L_1 + L_2 + L_3\right) = \left(\rho_{Water} g H_1 + P_{Atm}\right)\left(L_0 + L_1 + L_2 + L_3 + 2H_1 - H_{Rise}\right) \tag{8}$$

It is therefore possible to find the position of the water levels on both sides of the siphon pipe by solving for H_1 in Equation (8).

An important failure mode can also be identified from Equation (6) - that is, the height of water H_3 that will cause water to begin spilling over into the horizontal section of the siphon pipe. This is the maximum water height that the air trap can resist before failing, and it can therefore be used as a design constraint to select an appropriate vertical geometry of the siphon system. This failure mode takes place when H_2 goes to zero, so the maximum value of H_3 is found by subjecting Equation (6) to this condition and noting that when $H_2 = 0$, H_1 must be equal to H_{3Max}:

$$P_{Atm}\left(L_1 + L_2 + L_3\right) = \left(\rho_{Water} g H_{3Max} + P_{Atm}\right)\left(L_2 + L_3 + H_{3Max}\right) \tag{9}$$

Given the geometry of an SRSF siphon, Equation (9) can be solved for H_{3Max}, the maximum height of water that the air trap can support during a filtration cycle.

The siphon was evaluated experimentally in laboratory tests to validate this model. Following a backwash cycle, the water was allowed to rise in the column, and the locations of water levels in the siphon system were measured. Dimensions of the experimental siphon and the lengths measured during this experiment are shown in Figure 6.

For four different heights H_{Rise} of water in the column, the lengths a, b, and c were measured, and Equation (8) was solved to predict these lengths given the physical dimensions of the siphon in Figure 6(a). For these calculations, we used the dimensions of the apparatus $L_0 = 6\,cm$, $L_1 = 1.30\,m$, $L_2 = 16\,cm$, and $L_3 = 1.32\,m$, and an atmospheric pressure of $P_{Atm} = 1\,atm$. The results of this experiment are shown in Table 1. The measured values of a and c were the same at each point, as predicted by Equation (2), and the model underestimated the measured values of a, b, and c by 3-6%. The error in the predicted values comes from our estimate of the initial air volume in the siphon pipe - in reality, this initial air volume is larger than the volume shown in Figure 5(b), because the water passing through the U-shaped tube on the outside of the filter has momentum when the siphon is broken and it is expected to fall below the levels shown in the figure. However, our estimate of the initial air volume represents a minimum value, and it would therefore be appropriate to use the model for a conservative design.

Backwash siphon air valve sizing

The state of operation of the entire system is controlled by the air valve on the backwash siphon. This valve must accomplish two key functions. The first is to allow the air in the siphon air trap to escape when the filter is to be backwashed, as at the beginning of Zone B in Figure 4. The second is to break the siphon and pull in a new volume of air when backwash is finished and a new filtration cycle is to be started, as in Zone D.

The first function is readily accomplished. When the air valve is opened, the positive gauge pressure on the air trap forces the air to be quickly expelled into the atmosphere. To accomplish the second function, the air valve must allow a sufficient volume of air to enter so that the air trap can be re-formed in a reasonable amount of time. The desired flow rate of air to break the siphon and re-establish the air trap therefore sets the minimum required diameter of the air valve. The target air flow rate Q_{Target} of air is based on a desired time t_{Design} to fill the siphon:

$$Q_{Target} = \frac{V_0}{t_{Design}} \tag{10}$$

where V_0 is the initial air volume defined in Equation (4).

In addition to the target flow rate, sizing this valve requires that the relevant driving head and head losses be identified. The initial driving head h_0 in this situation is a result of the negative gauge pressure in the upper portion of the siphon during backwash:

$$h_0 = \Delta z_{Valve} + \frac{V_{Siphon}^2}{2g} + h_{LSiphon} \tag{11}$$

where Δz_{Valve} is the elevation of the air valve tee over the backwash water level in the filter column, V_{Siphon} is the flow velocity of water in the siphon, and $h_{LSiphon}$ is the head loss between the siphon entrance and the air valve tee. This equation is dimensionally consistent, as long as all lengths and head losses are expressed in consistent units (e.g. cm of water). When the air valve is initially opened there is a net pressure of h_0 forcing air into the system, but once the siphon pipe is filled with air, the pressure in the pipe approaches 1 atm and the driving head drops to zero. Therefore, the air valve should be designed for an initial flow rate of twice the target flow, because this will produce an average flow of Q_{Target} over a period of t_{Design}, given that the driving head will decline from h_0 to zero. Because minor losses dominate over the short length of the air valve pipe, the minimum size of the air valve D_{Valve} can be calculated with a minor loss equation:

$$D_{Valve} = \sqrt{\frac{Q_{Design}}{\pi}} \left(\frac{8K}{gh_{0Air}}\right)^{1/4} \tag{12}$$

where $Q_{Design} = 2Q_{Target}$; the coefficient K incorporates all minor losses along the path of air entering the system, including the air pipe entrance, the air valve itself, the air pipe exit, and any other adaptors or fittings; and h_{0Air} is the initial driving head h_0 from Equation (11) converted into units of air:

$$h_{0Air} = \left(\frac{\rho_{Water}}{\rho_{Air}}\right) h_{L0} \tag{13}$$

where ρ_{Air} is the density of air.

In the field, the goal to minimize air valve size was motivated by the desire to reduce construction costs. Using a wood board and hole saws to replicate the orifice size of standard ball valves, a series of tests were performed on the full-scale filter starting with a 3" PVC ball valve and covering the siphon opening with successively smaller orifices. The tested hole sizes included 2", 1 1/2", 1", 3/4", and 1/2" nominal pipe sizes. Both initiation and breaking of the siphon were tested to ensure that neither transition would fail due to insufficient air leaving or entering the siphon pipe. Successful termination of backwash was defined as having the water from the vertical section of the siphon pipe return to the filter box, indicating that the water in the siphon had been displaced by air.

Observations in the field showed that the air valve could be as small as a 1/2" brass ball valve (actual diameter 19/32" or 1.508 cm). No further testing was done with smaller valves, not only because the 1/2" valve met the goal of cost reduction and no smaller valve sizes were readily available, but also because the time to initiate and terminate backwash would be unacceptably long for smaller orifice sizes. The full-scale siphon has an air trap volume of approximately 44 L and a fill time of 5.6 s, yielding an average air flow rate of 7.8 L/s. The initial driving head of $h_0 = 1.25\, m$ of water for air flow into the full-scale siphon gives a K value of 2.65 in Equation (12). This is consistent with the nature of the minor losses in the system: the entrance to the air pipe could be thought of as a projecting entrance with $K = 1$, the exit from the air pipe into a much lower velocity zone would have an additional K very near 1, and there is some additional minor loss attributable to the open ball valve.

CONCLUSIONS

A novel system of fluidic controls has been developed for the SRSF to set its mode of operation, and this system has been successfully deployed at a municipal water treatment plant. The fluidic control mechanism is based on a siphon pipe controlled by an air trap, and on water level changes that are designed to automatically engage or disengage three inlets and three outlets. The use of a single small-diameter air valve to fill and empty the siphon with air simplifies operation and completely eliminates all of the failure modes associated with digital, electronic, and pneumatic controls that are common in mechanized water treatment plants. In addition, the cost of the air control valve is negligible in comparison with conventional digital, electronic, and pneumatic control systems. This novel system was tested in pilot-scale experiments, which demonstrated the transition between the filtration and backwash cycles. Physical models were proposed for the hydrostatics of the siphon air trap and for air flow in the control valve, and these models were validated by observations with the laboratory and full-scale systems.

ACKNOWLEDGMENTS

The authors thank Maysoon Sharif, Andrew Hart, Andrew Sargent, Sara Coffey, Min Pang, Ziyao Xu, and Alli Hill at Cornell University for their support of the research and design process, along with Sarah Long, Daniel Smith, Antonio Elvir, Roger Miranda, Jacobo

Nuñez, and Arturo Diaz at Agua Para el Pueblo in Tegucigalpa, Honduras for their work on this project in the field. We are also grateful to the members of the Támara municipal Water Board and to water plant operator Antonio Cerrato, who put significant time and resources into the first full-scale SRSF implementation. The laboratory work described in this paper was funded by grants from the U.S. Environmental Protection Agency P3 program, and the construction of the full-scale SRSF was financed by the Sanjuan Foundation and the Támara Water Board.

References

Adelman, M. J., Weber-Shirk, M. L., Cordero, A. N., Coffey, S. L., Maher, W. J., Guelig, D., Will, J. C., Stodter, S. C., Hurst, M. W., and Lion, L. W. (2012). "Stacked filters: a novel approach to rapid sand filtration." *Journal of Environmental Engineering*, in press.

American Society of Civil Engineers (ASCE) (2009). "2009 Report Card for America's Infrastructure." *Infrastructure Report Cards*, <http://www.infrastructurereportcard.org/report-cards> (May 24, 2011).

Breslin, E. D. (2003). "The demand-responsive approach in Mozambique: why choice of technology matters." *UNICEF-Waterfront*, 16, 9–12.

Foote, J., Baker, C., and Bordlemay, C. (2012). "Drinking water quality report." *Annual Water Quality Report 2012*, Bolton Point Municipal Water System, City of Ithaca Water System, and Cornell University Water System, <http://www.ci.ithaca.ny.us/departments/dpw/water/report.cfm>.

Hokanson, D. R., Zhang, Q., Cowden, J. R., Troschinetz, A. M., Mihelcic, J. R., and Johnson, D. M. (2007). "Challenges to implementing drinking water technologies in developing world countries." *Environmental Engineer: Applied Research and Practice*, 43, 31–38.

Lee, E. J. and Schwab, K. J. (2005). "Deficiencies in drinking water distribution systems in developing countries." *Journal of Water and Health*, 3(2), 109–27.

Moe, C. L. and Rheingans, R. D. (2006). "Global challenges in water, sanitation and health." *Journal of Water and Health*, 4, 41–58.

Onda, K., LoBuglio, J., and Bartram, J. (2012). "Global access to safe water: accounting for water quality and the resulting impact on MDG progress." *International Journal of Environmental Research and Public Health*, 9(3), 880–894.

Reynolds, T. D. and Richards, P. A. (1996). *Unit Operations and Processes in Environmental Engineering*. PWS Publishing Co., Boston.

Water Supply Committee of the Great Lakes (WSCGL) (2007). "Recommended Standards for Water Works." *Ten State Standards*, <http://10statesstandards.com/waterstandards.html> (June 18, 2012).

Weber-Shirk, M. L. (2009). "An automated method for testing process parameters." *Cornell University AguaClara*, <https://confluence.cornell.edu/display/AGUACLARA/Process+Controller+Background> (June 18, 2012).

Will, J. C., Adelman, M. J., Weber-Shirk, M. L., and Lion, L. W. (2012). "Implementation of the AguaClara stacked rapid-sand filtration process at the municipal water treatment plant in Tamara, Francisco Morazan, Honduras." *XXVII Congreso Centroamericano de Ingenieria Sanitaria y Ambiental*, San Salvador, El Salvador (March 2012).

List of Tables

Table 1. Predicted and measured values of a,b and c in the experimental siphon air trap, given H_{Rise}

H_{Rise} (cm)	a (cm)		b (cm)		c (cm)	
	Predicted	Measured	Predicted	Measured	Predicted	Measured
107.8	45.1	47.6	73.2	75.8	45.1	47.6
125.0	52.7	55.2	63.7	66.2	52.7	55.2
142.5	60.6	63.2	54.1	56.7	60.6	63.2
168.0	71.9	74.5	40.0	42.5	71.9	74.5

List of Figures

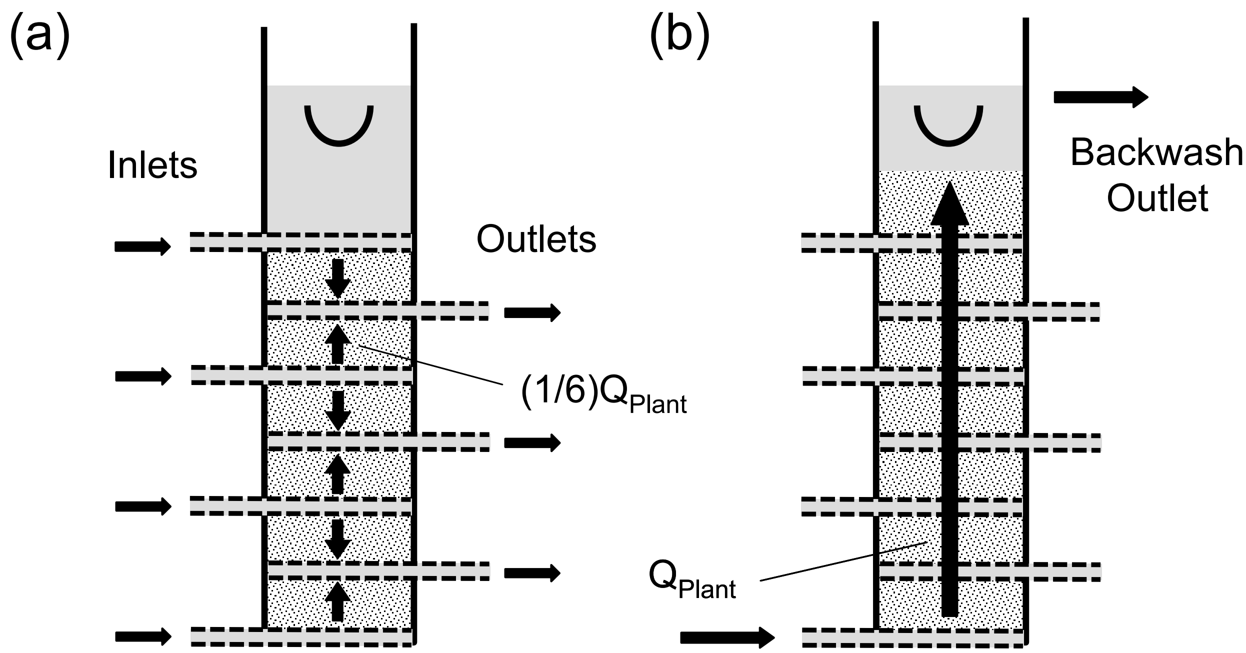

Figure 1. Diagram of flow in the sand bed of an SRSF during (a) filtration and (b) backwash. Note that the total incoming flow rate Q_{Plant} is the same during both cycles of operation.

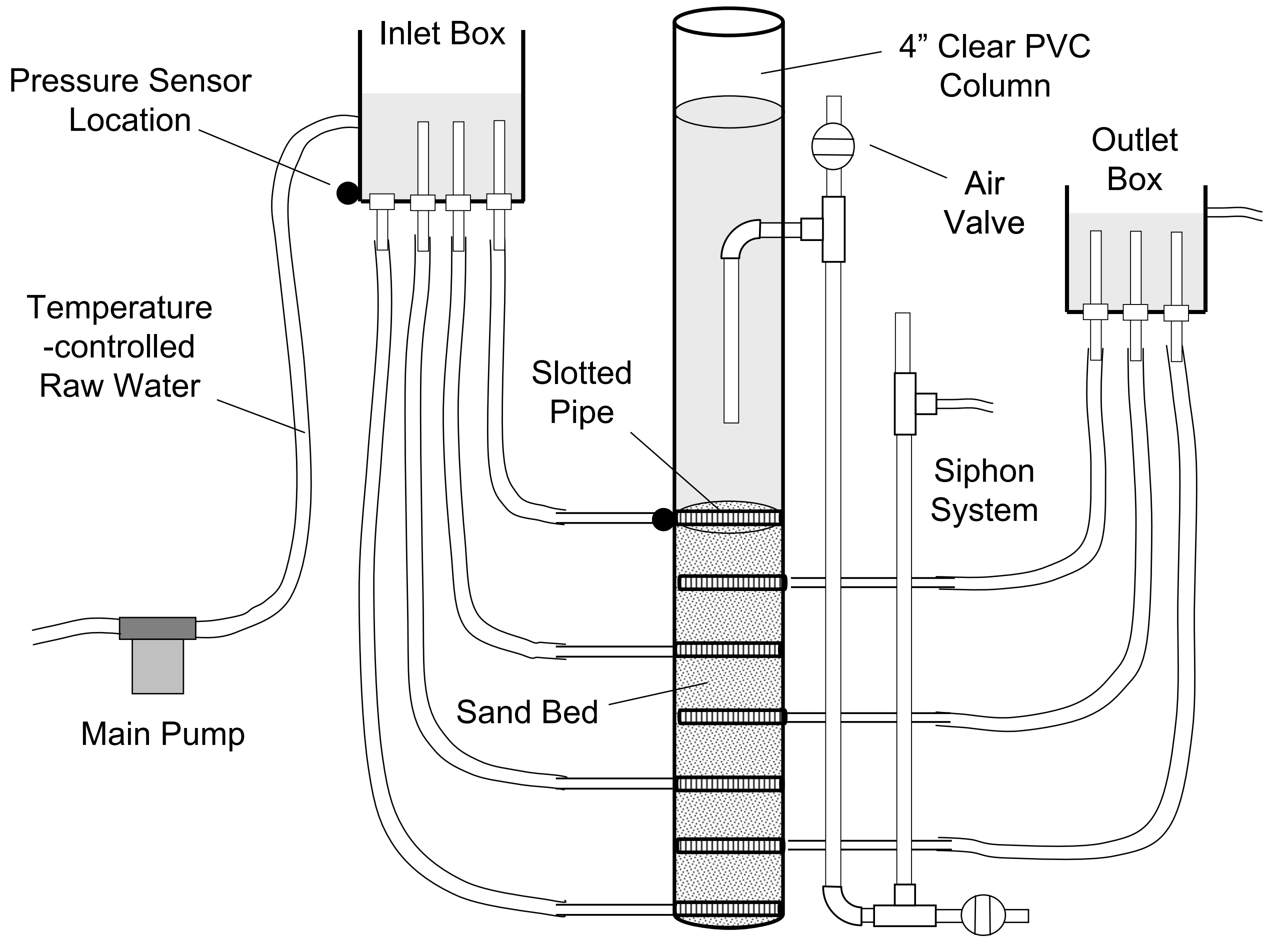

Figure 2. Pilot-scale experimental apparatus including an SRSF column, inlet and outlet boxes, a backwash siphon, an air valve, and pressure sensors. Note that the water levels shown here are for the filtration cycle.

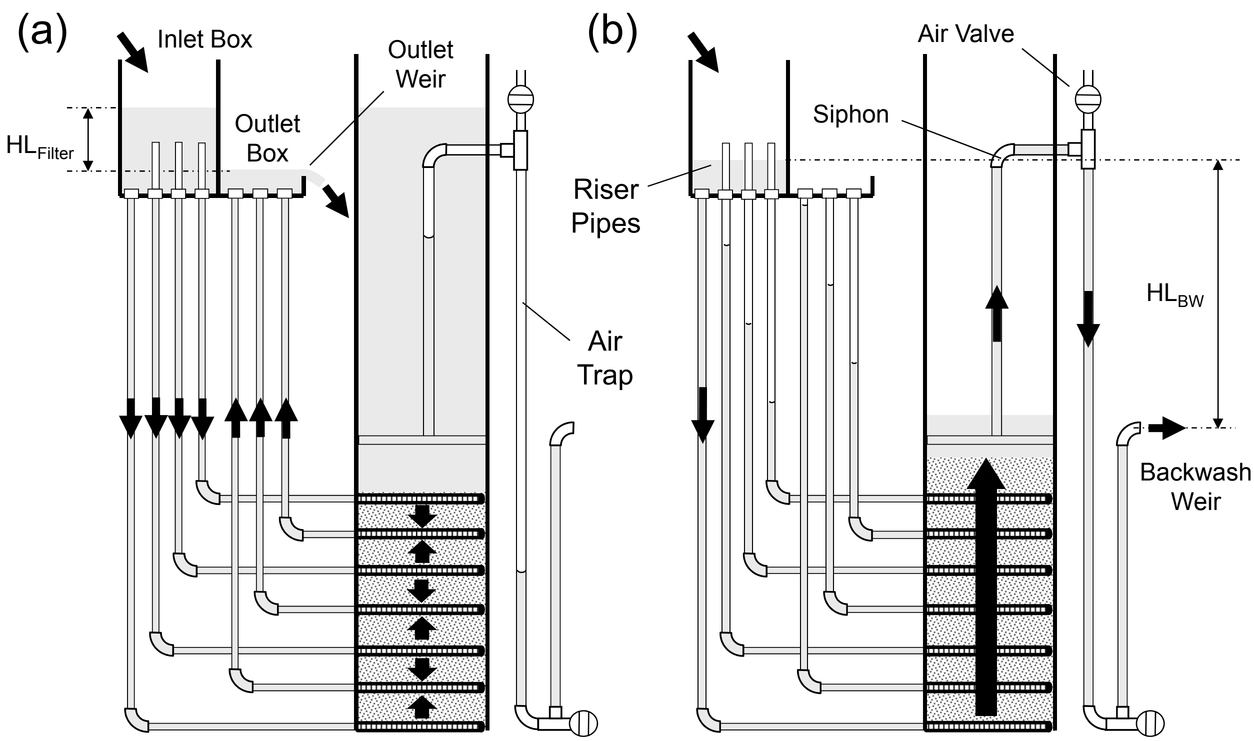

Figure 3. Fluidic control system for the SRSF, showing water levels during (a) filtration and (b) backwash. Important head losses during each cycle are also identified.

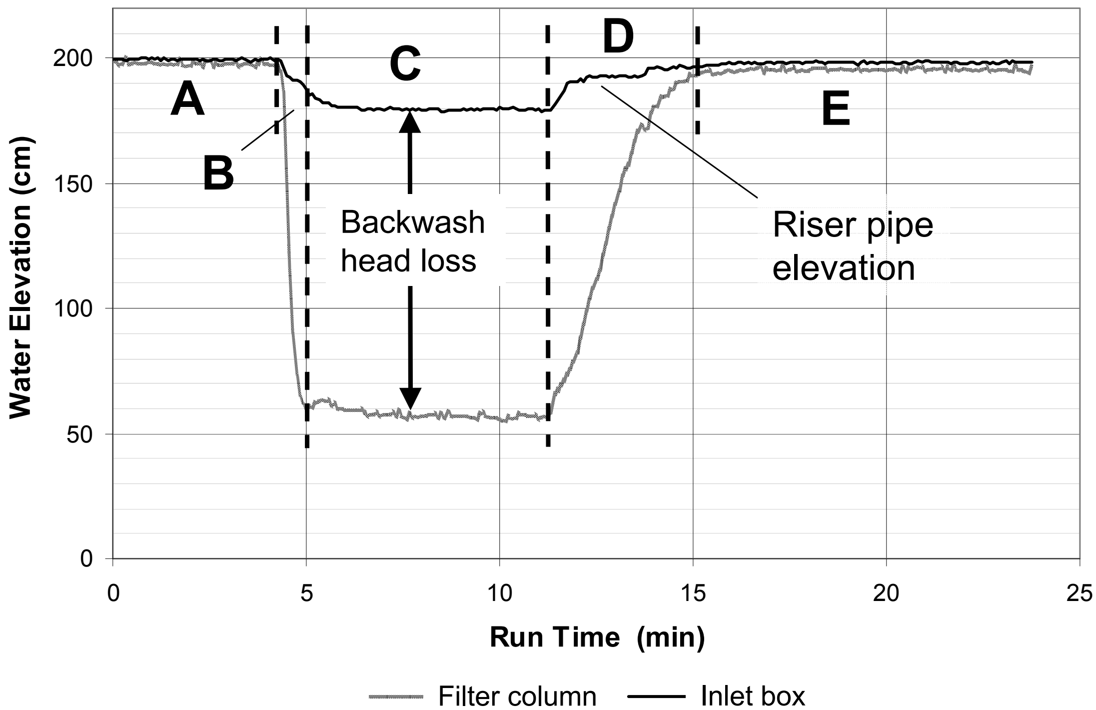

Figure 4. Water level traces from the pilot-scale apparatus, showing the water level change in the inlet box and the filter column during the transitions between modes of operation. The system starts in filtration mode (Zone A), transitions to backwash (Zone B), backwashes for five minutes (Zone C), transitions back out of backwash (Zone D), and returns to filtration (Zone E).

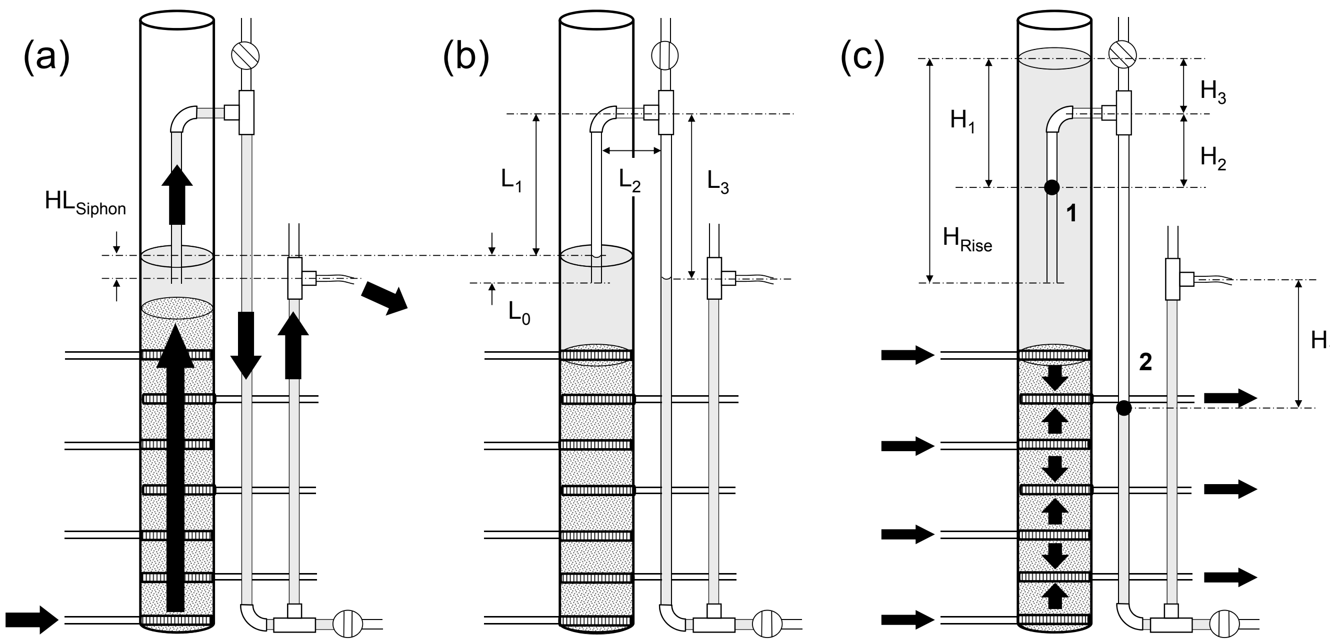

Figure 5. Diagram of water levels in the siphon pipe and key dimensions (a) during the backwash cycle, (b) just after the siphon is broken to end backwash, and (c) after water has risen to the clean-bed filtration height.

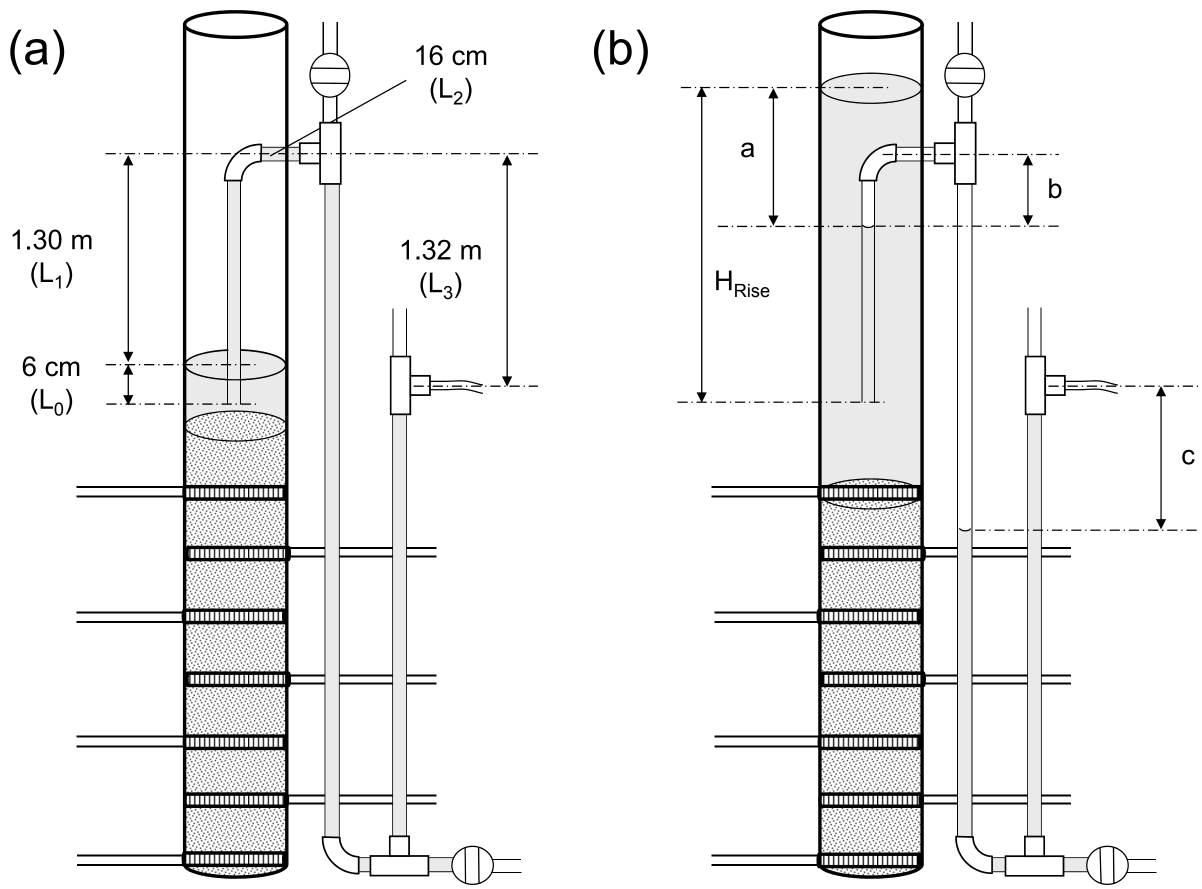

Figure 6. Diagram of (a) dimensions and (b) observed water levels for the laboratory-scale siphon system. The water in the filter column was allowed to rise a height H_{Rise} over the top of the sand, and the lengths a, b, and c were measured.